Coupled ocean-acoustic model studies of sound propagation through a front

A. D. Heathershaw and C. E. Stretch
Admiralty Research Establishment, Portland, Dorset DT5 2JS, United Kingdom

S. J. Maskell
University of Exeter, Exeter, Devon EX4 4QF, United Kingdom

(Received 14 September 1989; accepted for publication 7 September 1990)

A three-dimensional (3-D) numerical ocean model has been used to study sound propagation through an ocean front. The model has been used to provide environmental data for input to a range-dependent acoustic model to study the effect of eddies that form at the front on sound propagation characteristics. The model was set up in an idealized ocean domain but with the model physics and the temperature contrast across the front configured so as to represent the polar front east of Iceland. Acoustic ray tracing was carried out to illustrate the effect of frontal eddy features on sound propagation paths, and propagation loss calculations were performed to quantify their effect acoustically. It was found that dependent upon sound source/receiver depth combinations, the effect of the front and the eddies was to increase propagation loss by as much as 10–20 dB. This is comparable with the magnitude of the frontal effect that is seen in studies using analytical models of ocean fronts and with acoustic calculations that are based on measured environmental data. However, the results of this study have also shown that the acoustic predictions may be sensitive to the choice of ocean model parameter, in particular the horizontal eddy viscosity coefficient.

PACS numbers: 43.30.Cq, 43.30.Zk

INTRODUCTION

Ocean forecast models that are being developed for naval use will be required to resolve the ocean mesoscale variability due to fronts and eddies. It is well known that such features can have a significant effect on sound propagation leading in some cases to propagation loss increases of order 20 dB[1] and horizontal refraction effects[2] in excess of 1°. For the ocean modeler, there are two problems: Can the ocean model adequately represent the physical processes associated with fronts and eddies, and will such features be adequately resolved for acoustic purposes? The requirements of the acoustician may not necessarily be met by those of the ocean modeler.

Oceanographic processes may be parametrized and represented in ocean models at scales that are too coarse to resolve the acoustics. In the horizontal direction, subgridscale processes may be parameterized with eddy viscosity and diffusion coefficients, the values of which are more often chosen for numerical stability than for physical representativeness. In the vertical, ocean models may have insufficient resolution to resolve near-surface temperature gradients that, it is well known[3], can dramatically alter the way in which sound energy propagates in the upper ocean.

For naval forecast models, the solution, ultimately, will involve a "trade-off" between optimum resolution for the acoustics, and the computer power available to model a specific region of operational interest, e.g., the Atlantic or the Indian Ocean. Available computer power is increasing all the time so that the problem is likely to become less acute. In the meantime, however, it is important that we understand the sensitivity of the acoustic predictions not only to the environmental changes that the models predict, but also the model parameters.

Various attempts have been made to compare measured and predicted sound propagation characteristics for mesoscale features in the ocean. For example, Lawrence[4] has compared measured and predicted propagation loss characteristics for eddies in the Tasman Sea. These comparisons, however, were based on simplistic descriptions of the sound-speed structure of the eddies, relying on horizontal interpolation between characteristic profiles at the center and the edge of each eddy to enable a range-dependent propagation loss calculation to be made. A complete description of environmental conditions for acoustic purposes would require data sets that are over sampled and which could subsequently be subsampled to examine the effects of spatial resolution in the oceanographic variables describing the sound velocity field, i.e., temperature, salinity, and pressure. Such information is costly and time consuming to obtain and, for underwater acoustic studies, may not even be synoptic.

One solution is to run ocean and acoustic models together, to examine the sensitivity of acoustic predictions to changes in the oceanographic variables and to study their dependence on ocean model parameters. Previous studies of this type have concentrated on generalized models of oceanographic features such as fronts and eddies. For example, Henrick *et al.*[5,6] have developed an analytical model of mesoscale ocean eddies that relates acoustic properties to eddy size and strength, including currents. This model was subse-

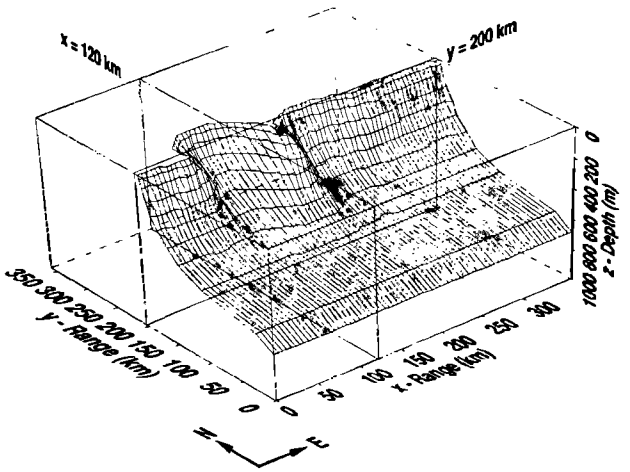

FIG. 1. Three-dimensional view of idealized frontal model showing position of 6 °C isothermal surface at 8 days following initialization with baroclinic step perturbation at front. Acoustic calculations have been performed on a section through the front at $x = 120$ km, and in a direction parallel to the front at $y = 200$ km.

quently used by Baer,[7] in conjunction with a 3-D acoustic model, to study horizontal and vertical refraction effects. Similarly, Rousseau *et al.*[8] have used an idealized model of an ocean front to study the dependence of short-range acoustic transmissions on frontal properties.

An inherent limitation of these studies has been their inability to evolve oceanographic features realistically in both space and time, for acoustic purposes. Some attempts[9,10] have been made to do this using 1-D numerical ocean models to study the effects of change in the upper ocean, although, until recently, little has been done with 3-D models to provide full environmental simulations for acoustic studies. There is now a growing body of research[11–14] on this topic and recently Mellberg *et al.*[15] have described the interfacing of the Harvard open ocean model[16] (HOOM) to a range-dependent acoustic model [IFD (Ref. 11)] to study the temporal variability of sound propagation through Gulf Stream eddies and meanders. However, the HOOM/IFD study[15] did not specifically address the problem of acoustic sensitivity to changes in ocean model parameters.

In this paper, we describe a coupled ocean-acoustic modeling technique that has been developed to address just this problem. A high-resolution 3-D numerical ocean model is used to simulate eddies at an ocean front and to provide synoptic estimates of the sound-speed structure throughout the frontal region. These have then been used as input to a range-dependent acoustic model. Some preliminary results are presented here that illustrate the sensitivity of the acoustic predictions to changes taking place at the front and which also demonstrate the potential of the technique for studying the sensitivity of underwater sound propagation characteristics to changes in ocean model parameters.

I. THE OCEAN MODEL

In this study, the ocean model has been configured so as to represent an idealized frontal system in a 3-D rectangular flat-bottomed ocean domain, with temperature contrasts and model physics appropriate to the polar front east of Iceland. The setup is shown in Fig. 1, which is a 3-D view of the frontal simulation with the model integrated for 8 days (see later).

The formulation that has been used in these studies is the Cox primitive equation model.[17] Other model formulations would be possible, e.g., quasigeostrophic models[16] and isopycnic coordinate models.[18] However, the Cox model is a robust and well-understood model, and is widely used in the ocean modeling community.

Following Cox, the equations for the conservation of heat, salt, and momentum are written, with the hydrostatic rigid lid and Boussinesq approximations, in spherical coordinates. For simplicity in later sections of this paper, in examining the model physics in relation to the acoustics, we consider the horizontal momentum equations in the x and y directions, written in Cartesian coordinates, viz.,

$$\frac{\partial u}{\partial t} + (\mathbf{q}\cdot\nabla)u - fv = -\frac{1}{\rho_0}\frac{\partial p}{\partial x} + A_H\nabla^2 u + A_V\frac{\partial^2 u}{\partial z^2}, \tag{1}$$

$$\frac{\partial v}{\partial t} + (\mathbf{q}\cdot\nabla)v + fu = -\frac{1}{\rho_0}\frac{\partial p}{\partial y} + A_H\nabla^2 v + A_V\frac{\partial^2 v}{\partial z^2}. \tag{2}$$

We also consider the temperature equation,

$$\frac{\partial T}{\partial t} + (\mathbf{q}\cdot\nabla)T = K_H\nabla^2 T + K_V\frac{\partial^2 T}{\partial z^2}. \tag{3}$$

It should be noted that in this study a single tracer version of the Cox model was used in which temperature only is modeled. Salinity is assumed constant and density is computed using a linear equation of state.

In Eqs. (1)–(3), u and v are the horizontal velocity components in the x and y directions, p is the pressure, ρ_0 is the reference density, and f is the Coriolis parameter. Here, T is the temperature and t is time. Also, x and y are measured west–east and south–north as shown in Fig. 1, and z is measured vertically upward. Here, $\mathbf{q}$ is the fluid particle velocity $\mathbf{q} = (u,v,w)$, where w is the vertical velocity component; ∇ is the operator $(\partial/\partial x, \partial/\partial y)$. Also, A_H and A_V are the horizontal and vertical eddy viscosity coefficients and K_H and K_V are the horizontal and vertical eddy diffusion coefficients. These quantities are discussed later in relation to the acoustic calculations.

For the simulations described here, the spherical-coordinate equivalents of Eqs. (1)–(3), together with the hydrostatic and continuity equations, and a linear equation of state, are solved in finite difference form on an Arakawa B-grid, with a leap-frog time-stepping scheme. Further details of the method of solution may be found in Cox[17] and in Heathershaw *et al.*[19]

The model is set up with 15 levels in the vertical for

which $\Delta z = 25$ m in the top two levels and $\Delta z = 75$ m in each of the remaining 13 levels, giving a total depth of 1025 m. The horizontal range increments were $\Delta x = \Delta y = 5$ km with a total of 72 increments in the x and y directions, respectively, giving overall dimensions of 360×360 km. The time step chosen for these particular simulations was $\Delta t = 360$ s. This value was found to give numerically stable solutions for the type of calculation performed here. At larger values of Δt, it was found that the fields predicted by the model became "noisy." For the bulk of the simulations described here, the horizontal and vertical eddy viscosity coefficients, A_H and A_V, are set to 1.0×10^7 and 1 cm^2 s^{-1}, respectively, and the horizontal and vertical eddy diffusion coefficients (K_H, K_V) are 1.0×10^5 and 1 cm^2 s^{-1}. However, for the acoustic investigations that follow, A_H and K_H have also been varied within prescribed limits.

The ocean model domain was initialized with an east–west front having a temperature difference across the front of approximately 3.3 °C. The temperature field, with constant salinity (35‰), was used to calculate an initial zonal current field by integrating the thermal wind equation, $\partial u/\partial z = (g/f\rho)(\partial \rho/\partial y)$. The front was then perturbed by introducing a baroclinic instability at the front, resulting in meandering and eddy formation. However, it should be noted that the initial current field was not in complete geostrophic balance, a small out of balance component occurring as a result of integrating the thermal wind equation in Cartesian coordinates, but performing the simulations in spherical coordinates. A further imbalance occurs as a result of the initial baroclinic disturbance being applied to the temperature field only. The initial adjustments to these nongeostrophic perturbations resulted in inertia-gravity waves that were quickly damped by the semi-implicit scheme used for the Coriolis term (Cox[17]). Once the model was running, with the short time step used, it was found that implicit or explicit schemes could be used (Wood[20]). Lateral boundary conditions for the model were cyclic in the E–W direction and in the N–S direction could be closed, i.e., zero normal flow, or open. In the latter case, open boundary conditions were applied using the method of Stevens.[21] Since the flow in these experiments was initially zonal, i.e., from west to east, the results of the simulations with the N–S boundaries open were not significantly different from those with the boundaries closed.

As stated, in this study, the model has been used to generate eddies by introducing a baroclinic perturbation over a region of the front. This was achieved by increasing the temperatures by 1 °C in the top 300 m of the water column along a 55-km section of the front centered on $x = 87.5$ km. The model was then integrated forward in time to generate eddy-like features at the front.

It should be noted that the model has no external forcing, i.e., no wind stress at the sea surface, and no buoyancy due to surface heating. Thus the boundary conditions on velocity and temperature at the surface ($z = 0$) are that $\partial u/\partial z$, $\partial v/\partial z$, and $\partial T/\partial z$ are all zero. Similarly, there is zero drag applied at the ocean floor, i.e., $\partial u/\partial z$, $\partial v/\partial z$ are zero at $z = -H$, where H is the total depth, and also $\partial T/\partial z$ is zero, i.e., there is no heat flux through the ocean bed. In the context of the coupled ocean-acoustic simulations that are described here, the ocean model is used as a process model to investigate the sensitivity of acoustic predictions to changes in the environment and in ocean model parameters. For this purpose, we have concentrated on a section through the front at $x = 120$ km, and a section along the front at $y = 200$ km. The locations of these sections are shown in Fig. 1.

The numerical model described in these studies is an adaptation of the Cox model,[17] vectorized for running CYBER and CRAY machines. For the bulk of the computations described here, the model has been run on a VAX 8700 machine, requiring nearly 76 min CPU time for a 1-day simulation in extended precision. For long integration periods (8 days), the model was run on a CRAY 1-S machine, requiring only 2 min 39 s CPU time per model day. Further details of these tests are given in Cooper.[22]

II. THE ACOUSTIC MODEL

To investigate the acoustic significance of changes in the ocean environment, we have used the eddy resolving model described above to generate environmental data for input to a range-dependent acoustic model.

The acoustic model that has been chosen for these studies is GRASS (Germinating Ray-Acoustic Simulation System), a range-dependent ray theory model capable of producing ray trace diagrams and frequency-dependent propagation loss curves. The primary use of the model in this study has been to investigate the way in which sound propagation characteristics are influenced by frontal eddy features and to study the dependence of the acoustic predictions on ocean model parameters. Further details of GRASS may be found in Cornyn[23] and Harrison.[24]

Salinity and temperature values at 5-km intervals and at each of the ocean model levels, were used to calculate sound velocity profiles using Chien and Millero's equation.[25] Smooth profiles were fitted to these data using a cubic spline to give continuous first- and second-order derivatives (see Cornyn[23]). A total of 72 profiles was therefore available for ray tracing, with linear interpolation between profiles being used to obtain sound-speed values at intermediate ranges. The range increment employed in GRASS, when ray tracing, is variable and adjusts automatically to minimize the time spent in calculating ray paths. Thus, while the increment will be small in regions having strong vertical gradients, e.g., below the warm layer on the south side of the front (see Fig. 1), at depth, where the gradients are weaker, the step size will be large.

For ray tracing to study sound propagation paths in the frontal region, a total of 11 rays was used with rays being launched at 1° intervals in a range of angles $\pm$ 15° about the horizontal. For propagation loss calculations, GRASS permits up to 1500 rays to be traced with the number being increased until a convergent solution is obtained for the intensities. In this study, convergence was obtained with a ray density of 48 rays per degree in a range of angles $\pm$ 15° about the horizontal, giving a total of 1440 rays.

To calculate propagation loss, each ray was attenuated

by a factor $e^{-\alpha R}$ where α is a frequency-dependent attenuation coefficient in dB per km and R is the range to the receiver. Values of α may be specified or can be calculated independently as a function of frequency using Thorp's formula.[26] In this study, a value of α of 6.57×10^{-2} dB km^{-1} has been used, calculated from Thorp's formula and corresponding to a frequency of 1 kHz. It was assumed that rays striking the sea surface were specularly reflected without loss, and rays striking the ocean bottom were fully absorbed. GRASS permits a range-dependent bottom loss to be specified, but in this study, so as to isolate effects due to changes in the water column, all bottom interactions have been suppressed.

An omnidirectional source was assumed with the rays confined between the angular limits given above. Ray amplitudes were set to unity and the intensity at the receiver calculated by assuming phase-independent contributions from individual rays arriving at the receiver (see Cornyn[23] for further details).

The source depth chosen for these studies was 100 m, placing it within the warm layer on the south side of the front when considering propagation from that direction, while receiver depths of 100 and 250 m were chosen to illustrate the variations in sound intensity for a receiver situated within an eddy and for one positioned just below it.

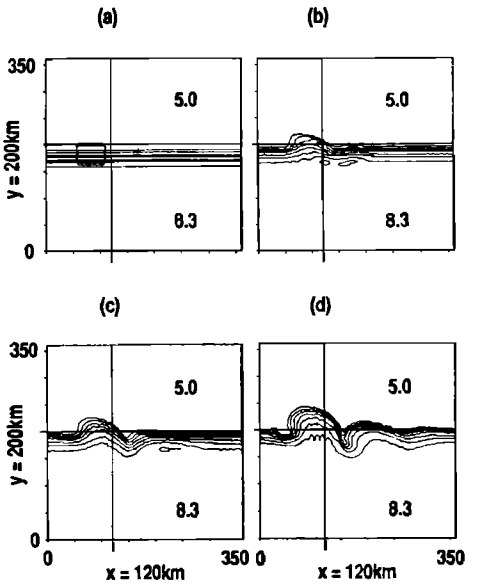

FIG. 2. Evolution of the near-surface temperature field ($z = -12.5$ m) at 2, 4, and 8 days [Fig. 2(b)–(d), respectively]. Figure 2(a) shows the location of the initial baroclinic step perturbation, centerd on $x = 87.5$ km and of length 55 km in the along-front direction. For these simulations, the horizontal eddy viscosity, A_H, has been set to 1×10^7 cm^2 s^{-1}. $K_H = 10^5$ cm^2 s^{-1} and A_V and K_V are 1 cm^2 s^{-1}, respectively.

III. RESULTS

The results of the frontal simulations with the ocean model are shown in Figs. 1–4. Figure 1 illustrates the three-dimensional structure of the front at 8 days following the initial disturbance, while Fig. 2 shows the near surface ($z = -12.5$ m) temperature field at 0, 2, 4, and 8 days. This indicates a wavelike disturbance spreading toward the east, which after 8 days [Fig. 2(d)] has the characteristic eddy shape that is seen in satellite images of the frontal region east of Iceland (Heathershaw *et al.*[20]). The form of the initial baroclinic disturbance that is used to generate eddies is shown at Fig. 2(a).

The eddy structure of the front becomes more apparent with longer integrations and Fig. 3 shows the near-surface temperature field at 24 days. This Figure also indicates the variation in horizontal current structure throughout the frontal region. Henrick *et al.*[6] have shown that currents may be important for sound propagating through eddies, causing horizontal refraction of the sound propagation paths.

Temperature sections through and along the front, at 8 days following the initial disturbance, are shown in Fig. 4. It should be noted that detached eddies, as indicated by closed circulation paths in the simulated current fields (Fig. 3), do not appear until after about 20 days. Thus the features that appear in vertical sections along the front [e.g., Fig. 4(b)], although having the appearance of detached eddies, are in fact due to small N–S displacements of the front about an E–W section. However, since we can only consider sound propagation in two dimensions, we shall in future refer to these features as "eddies."

Figure 4(a) shows the classic two-layer thermal structure of the front which, for the polar front east of Iceland, corresponds to warm North Atlantic water overlying cold Norwegian Sea water. Little vertical structure exists within these layers because none was present in the initial profiles, i.e., each layer was assumed to be isothermal. Despite this, the general appearance of the front is in good agreement with

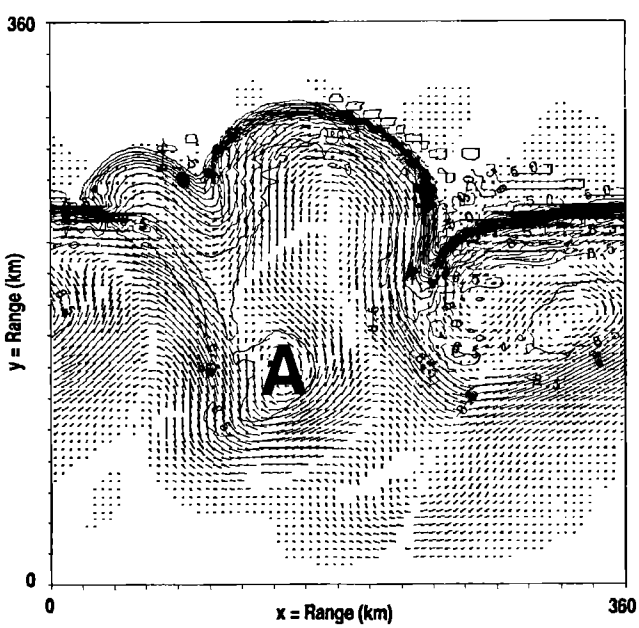

FIG. 3. Simulation of the near-surface ($z = -12.5$ m) current and temperature fields at 24 days following initialization with a baroclinic perturbation. Here A_H, A_V, K_H, and K_V values are as for Fig. 2. Nonlinear processes at the front are beginning to lead to the appearance of detached eddy features ("A") as shown by "closed" circulation paths in the currents.

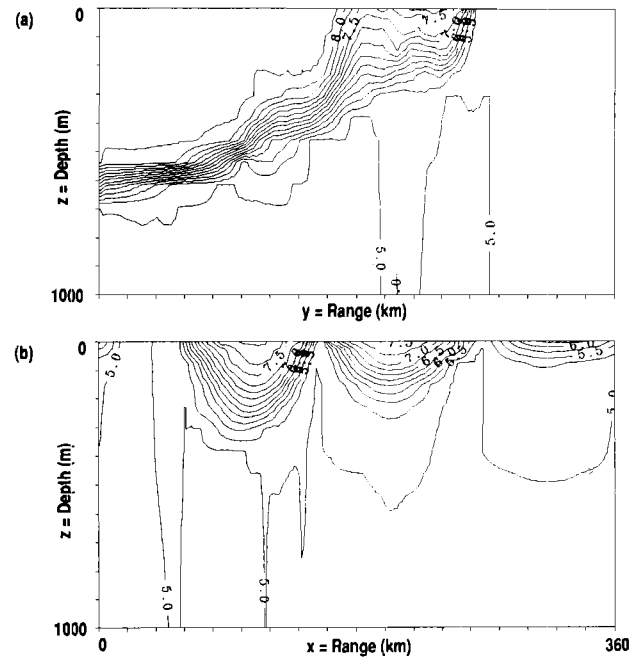

FIG. 4. Temperature sections through (a) and along (b) the front for the sections at $x = 120$ km and $y = 200$ km as shown in Fig. 1. Results are shown for 8 days following initialization with a baroclinic perturbation and with A_H, A_V, K_H, and K_V as for Fig. 2.

the results of high-resolution thermistor chain measurements in the Iceland–Faeroes front region (Scott and McDowall[27]) and with open ocean fronts in general. Further work is in progress to enable a more realistic description of the initial temperature fields.

Figures 5 and 6 illustrate the results of ray tracing on sections through and along the front at $x = 120$ and $y = 200$ km, respectively (see Fig. 1), with the sound source at a depth of 100 m and positioned at opposite ends of each section. Figure 5 shows that with the sound source placed in the warm water on the south side of the front, sound energy travels in a deep surface duct as far as the front, and is then refracted downward into the colder and acoustically slower polar water to the north of the front. With the sound source to the north, little sound energy penetrates the warm surface layer and is refracted downward beneath it. Figure 6 clearly illustrates the effect of mesoscale disturbances at the front on sound propagation paths and shows that sound energy may be deflected downward by up to 300 m beneath the eddylike features that are illustrated in Fig. 4(b). These features are, in effect, anticyclonic warm-core eddies with acoustically faster water at their centers. Typically, a sound-speed change of 10 ms^{-1} is associated with eddy features of the type that are shown in Fig. 4(b). From Fig. 6, the broad pattern of disturbance to the sound propagation paths is similar whether considering sound propagating from west to the east or vice versa.

Coupled ocean-acoustic simulations of the type described here, enable the temporal variations in sound propagation characteristics in frontal regions to be studied. For the baroclinic perturbation case described here, we have found that through-front propagation characteristics are altered little in the early stages of frontogenesis. For periods out to 8 days (Fig. 2), the only observed changes were a gradual broadening of the convergence zones that appear (Fig. 5) in the cold water on the northern side of the front when the sound source is in the warm water layer to the south. This is associated with a weakening of the horizontal temperature gradients on the cross-frontal section at $x = 120$ km, (see Figs. 1 and 2), as the front becomes more diffuse in this region. At other locations, temperature gradients might actually be strengthened, giving different acoustic propagation characteristics. Few other generalizations are possible in this study regarding the behavior of convergence zones because we have assumed a fully absorbing bottom for rays striking the seabed.

In contrast, sound propagation characteristics in directions parallel to the front, over the section at $y = 200$ km, were found to vary considerably during the initial stages of growth of frontal features. This result is not surprising as only small displacements of the front are required to induce large changes in the along-front temperature and sound velocity fields. The observed changes in the sound propagation paths will also depend critically on where these sections are taken in relation to the front. In general, perturbations in the sound velocity field and the sound propagation characteristics, will be greatest when the displacement due to a mesoscale feature is at right angles to the sound propagation path.

Corresponding to the temperature sections shown in Fig. 4, propagation loss curves were calculated for a frequency of 1 kHz and with the acoustic model parameters described previously. Source depth/receiver depth combinations of 100/100 and 100/250 m were used, the latter to illustrate differences that would occur with the receiver placed just below the eddy feature shown in Fig. 4. For both the across- and along-front cases (i.e., sections at $x = 120$ and $y = 200$ km), a range-independent propagation loss curve was calculated. This was obtained by taking the first temperature profile in the modeled section and assuming uniform conditions down range of this. The results of these calculations are shown in Fig. 7(a) for a source/receiver depth combination of 100/100 m only.

With the ocean model integrated for 8 days, the most striking feature of the results for propagation through the front is the 15-dB average increase in propagation loss that occurs with the source at 100 m, as sound travels from the warm side of the front to the cold. Beyond this, fluctuations of about 10 dB occur as a result of the convergence zone behavior described previously (see Fig. 5). With the receiver at 250 m, Fig. 7(a) shows that the frontal effect is less pronounced but still equivalent to about 5 dB.

For the section along the front at $y = 200$ km, Fig. 7(b) shows a 20-dB increase in propagation loss, when compared to the range-independent case, which can be associated with eddylike features at the front. With the receiver at 250 m, the effect of the eddies is less pronounced.

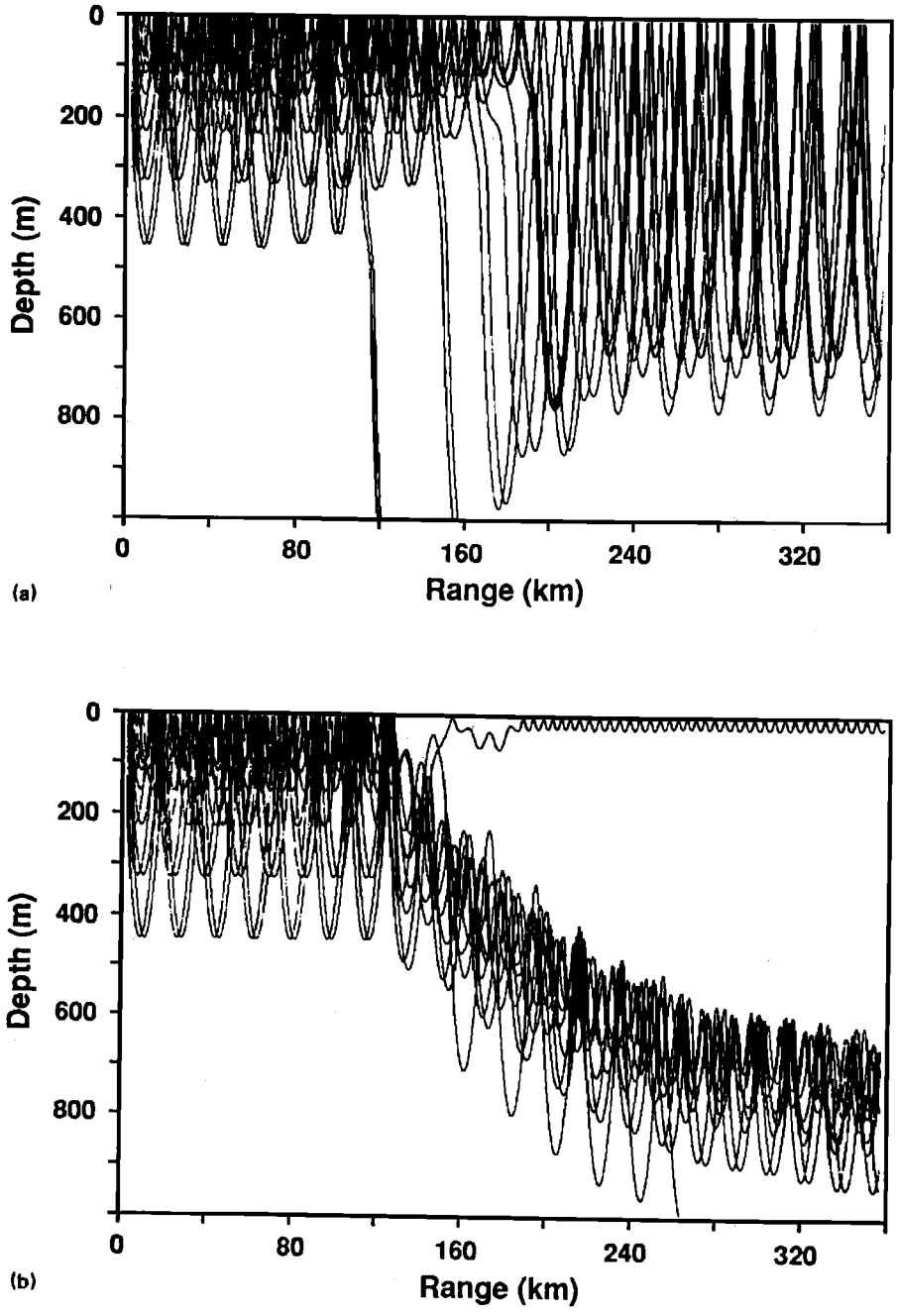

FIG. 5. Ray trace diagrams for the through-front section at $x = 120$ km (see Fig. 1) and (a) with the sound source in warm water to the south of the front and (b) with the sound source in cold water to the north. In both cases, the sound source has been placed at a depth of 100 m. These results correspond to the temperature section shown in Fig. 4(a).

IV. DISCUSSION

In studying the effects of mesoscale variability on underwater sound propagation characteristics, it will always be necessary to obtain *in-situ* measurements at sea, both of sound propagation and the oceanographic variables. However, measurements at sea can be costly and time consuming and even then can only tell us how things were on the day the measurements were made, i.e., they are of little use in predicting future states. Measured oceanographic fields may also lack synopticity, as mentioned previously.

Computer models on the other hand provide a cost effective means of studying oceanographic processes under well-controlled conditions and in a physically consistent manner. Thus it is possible to assess the acoustic significance of ocean fronts having different temperature contrasts or to determine the effect on sound propagation of eddies having different dimensions. A further advantage is that an ocean model may be coupled together with an atmospheric model to predict the future state of the ocean, at least in the upper layers. A variety of experiments is therefore possible, in which spatial and temporal variability can be introduced into the problem in a way that would be difficult to achieve with measurements alone.

The benefit of this approach for naval oceanographers who are developing ocean forecast models, is that it is possi-

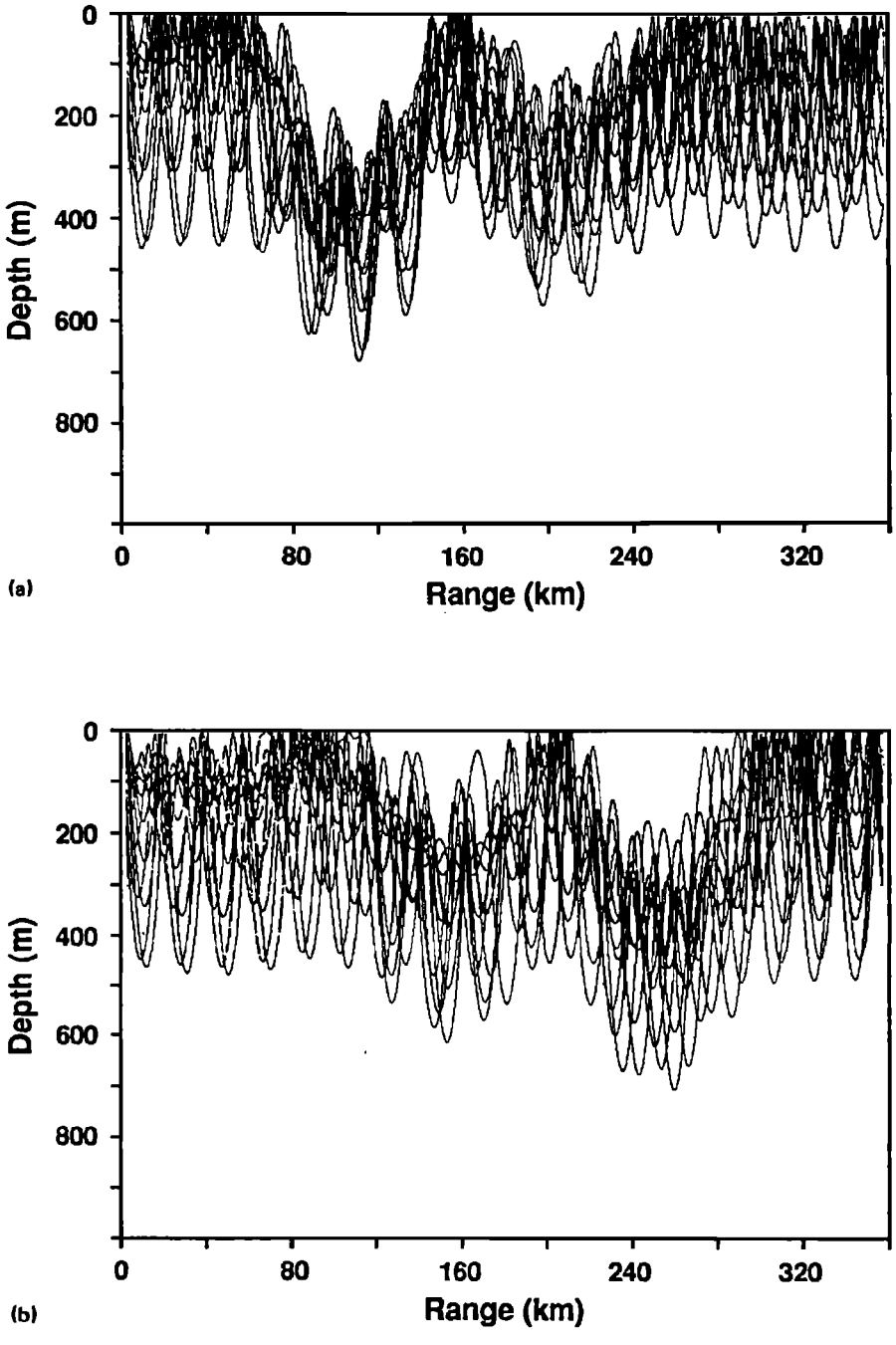

FIG. 6. Ray trace diagrams for the along-front section at $y = 200$ km (see Fig. 1) and with the sound source on the western (a) and eastern (b) boundaries of the front. The sound source has been placed at depths of 100 m. These results correspond to the temperature section shown in Fig. 4(b).

ble to assess the acoustic significance of a range of oceanographic features for which no measurement-based analogs exist. Measurements can always supplement this information and, in particular, are required to confirm the model physics. However, models offer a quicker and cheaper solution to the problem.

To do this effectively, we need good ocean models and good acoustic models. This study has shown that it is possible to combine a 3-D dynamical ocean model with a range-dependent 2-D acoustic model to give realistic simulations of the effects on an ocean front on underwater sound propagation characteristics. In particular, a high-resolution primitive equation ocean model has been used to simulate mesoscale eddy features at an ocean front, and a range-dependent ray theory acoustic model (GRASS) has been used to quantify their effect acoustically.

The ocean model that has been used in this study is highly idealized. The model physics are described in a rectangular flat-bottomed ocean domain with no heating, cooling, or wind mixing at the sea surface and with no representation of topographic features such as the Iceland–Faeroes Ridge. Clearly the model is unable to show the effects of bathymetry

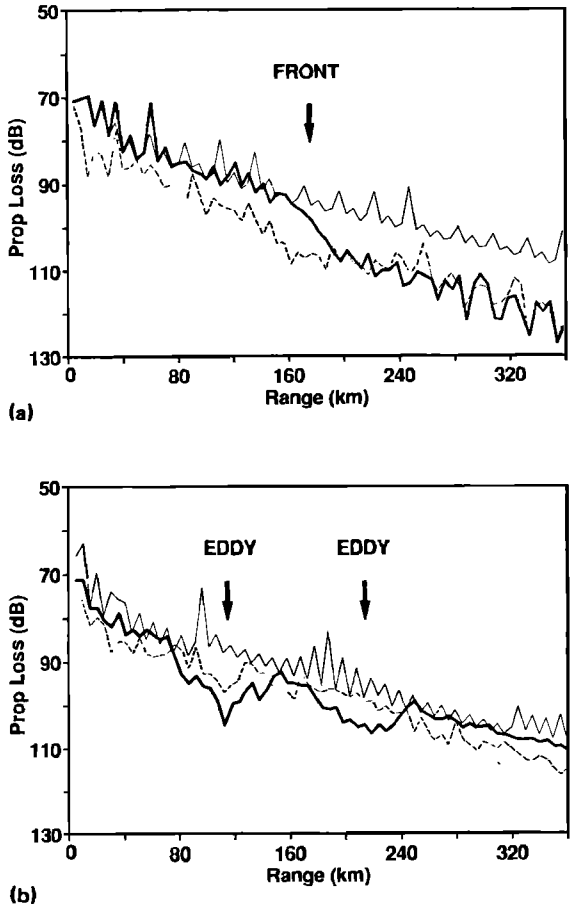

FIG. 7. Propagation loss curves (a) through the front at $x = 120$ km and (b) along the front at $y = 200$ km. Results are shown for sound source/receiver dispositions of 100/100 m (thick line) and 100/250 m (broken line). The results of a "range-independent" calculation are also shown (thin line), assuming the temperature profile at $x = 0$ and $y = 0$ to apply over the whole range. These calculations were performed on the ocean model simulations at 8 days following the initial baroclinic disturbance and with A_H, A_V, K_H and K_V equal to 10^7, 1, 10^5 and 1 cm^2 s^{-1}, respectively.

and coastlines, although work is in progress on another version of the model in which this will be possible.

How realistic then is our ocean model, in particular is it dynamically correct and does it predict the correct wavelengths and rates of growth for the observed frontal features? To examine this aspect, tests were performed perturbing the model with different wavelength features at the front and comparing the rates of growth of these features with the values predicted by theory. For a two-layer model of a front, Killworth *et al.*,[28] predict maximum growth rate to be at a wavelength $2\pi R_i$, where R_i is the internal Rossby radius given by

$$R_i = f^{-1}(g'h)^{1/2}, \tag{4}$$

where h is the depth of the warm layer, in a two-layer model of the front, g is the acceleration due to gravity, f is the Coriolis parameter, and g' is the reduced gravity given by $g' = g(\rho_2 - \rho_1)/\rho_2$, ρ_1 and ρ_2 being the densities of the upper and lower layers, respectively. For the setup studied here, $h = 500$ m, $\rho_2 = 1027.92$ kg m^{-3} and $\rho_1 = 1027.10$ kg m^{-3}, which for a latitude of 65 °N, appropriate to the Iceland–Faeroes front, gives $R_i \simeq 15$ km and maximum growth rate at a wavelength of $2\pi R_i = 94$ km.

Tests were performed by imposing initial small amplitude sinusoidal displacements, at the front, with wavelengths in the range 0.25–1.4 times the maximum growth rate wavelength given above. These tests were performed for A_H values in the range 2×10^7 cm^2 s^{-1} to 0.1×10^7 cm^2 s^{-1}. Growth rates were calculated using a centered difference approximation to $(d/dt)(\log A)$, where A is the amplitude of the wave. At a value of A_H equal to 0.25×10^7 cm^2 s^{-1} the initial growth rates agreed well with the values obtained by Killworth *et al.*,[28] all nonzero growth rates lying within 11% of their results. Full details of these tests can be found in Wood.[15]

In a second set of experiments, the results of which have been used in this study for acoustic investigations, the front was perturbed with a baroclinic disturbance of the type described previously. These tests were performed with the range of A_H values described above, and with K_H, A_V, and K_V constant at 10^5, 1 and 1 cm^2 s^{-1}, respectively. The model was integrated for periods of 2, 4, and 8 days and the growth of the frontal features observed. The inital disturbance was found to have the characteristic backward breaking wave form due to baroclinic instabilities (Dippner[24]) and which results from the "jet" (Fig. 3) that runs along the front from west to east. (The outer parts of the disturbance are in effect left behind by the faster moving region at the center and closer to the front.)

For the baroclinic perturbation and for all the cases of A_H examined, the initial disturbance has a wavelength of about 90 km at 2 days, slightly less than, but close to, the preferred wavelength of 94 km. At 4 days the wavelength is 120 km and at 8 days, between 110 and 120 km, although by this time the dynamics is fully nonlinear, and the linear analytical theory[28] is only indicative. The results with the model integrated to 8 days and for different A_H values are shown in Fig. 8.

While the ocean model may be dynamically correct in terms of the wavelength of the feature at the front having maximum growth rate, are the differences in detail of the model predicted fields significant acoustically? The results in Fig. 8, with A_H varied in the range $0.1\text{-}2\times10^7$ cm^2 s^{-1} but with K_H, A_V, and K_V constant, show that the lowest value of A_H [Fig. 8(a)] gave noisy results, while the highest value [Fig. 8(d)] gave results in which the growth rate was reduced, although the spatial scales were similar in all cases. A similar study of the effect of varying K_H was also carried out and this showed (Fig. 9) that there was little discernible difference in the modeled fields at 8 days.

The effect of the choice of A_H values in Eqs. (1) and (2) can be seen if we consider the effect of the eddy viscosity term in the simplified momentum equation:

$$\frac{\partial u}{\partial t} = A_H \frac{\partial^2 u}{\partial x^2}, \tag{5}$$

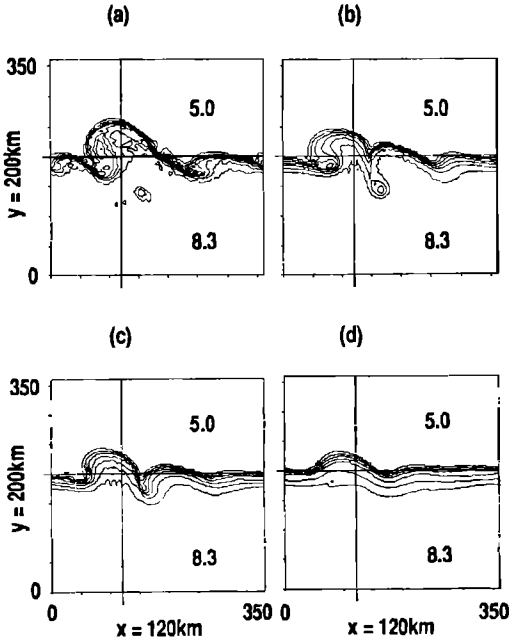

FIG. 8. Ocean model simulations of the near-surface ($z = -12.5$ m) temperature field at 8 days following the initial baroclinic disturbance at the front and illustrating the effect of varying the horizontal eddy viscosity A_H. Results are shown for A_H values of (a) 0.1×10^7, (b) 0.5×10^7, (c) 1×10^7, and (d) 2×10^7 cm^2 s^{-1}, respectively, but with K_H, A_V, and K_V held constant at values of 10^5, 1, and 1 cm^2 s^{-1}, respectively.

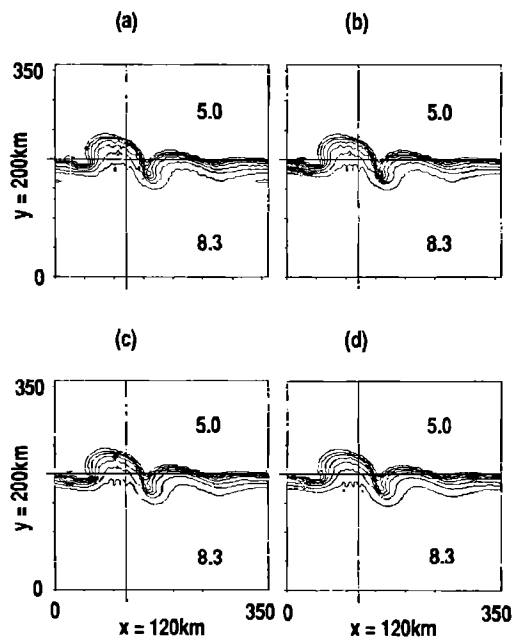

FIG. 9. Ocean model simulations of the near-surface ($z = -12.5$ m) temperature field at 8 days following the initial baroclinic disturbance at the front and illustrating the effect of varying the horizontal eddy diffusion coefficient K_H. Results are shown for K_H values of (a) 0.1×10^5, (b) 0.5×10^5, (c) 1×10^5, and (d) 2×10^5 cm^2 s^{-1}, respectively, but with A_H, A_V, and K_V held constant at values of 10^7, 1, and 1 cm^2 s^{-1}, respectively.

where u is the horizontal velocity in the x direction (the same arguments would apply to the y-momentum equation). Consideration of the dimensions of Eq. (5) gives a relation between length (L) and timescales (T) of the form $T = L^2/A_H$, where T, in effect, is the timescale on which an oceanic feature of lateral extent L is damped.

Thus, with $A_H = 1\times10^7$ cm^2 s^{-1}, Eq. (5) gives a characteristic "spin-down" time for an ocean eddy of diameter 30 km, of about 16 days. This is longer than the timescales of interest in operational ocean forecast models, which typically will be of order 1–4 days, and suggests that provided the models are updated with information at this frequency, the broad level of detail of mesoscale features that is input to an ocean model, will be retained in the forecast model fields.

The question remains, however, as to the acoustic significance of the detailed changes that are shown in the ocean model simulated fields at Fig. 8. To assess this problem, we have performed propagation loss calculations on the sections described previously, both through and along the front, for all four values of A_H, and with the same acoustic model parameters as before. The results of these calculations are shown in Fig. 10 and suggest that for sound propagating through the front [Figure 10(a)], there will be an uncertain-

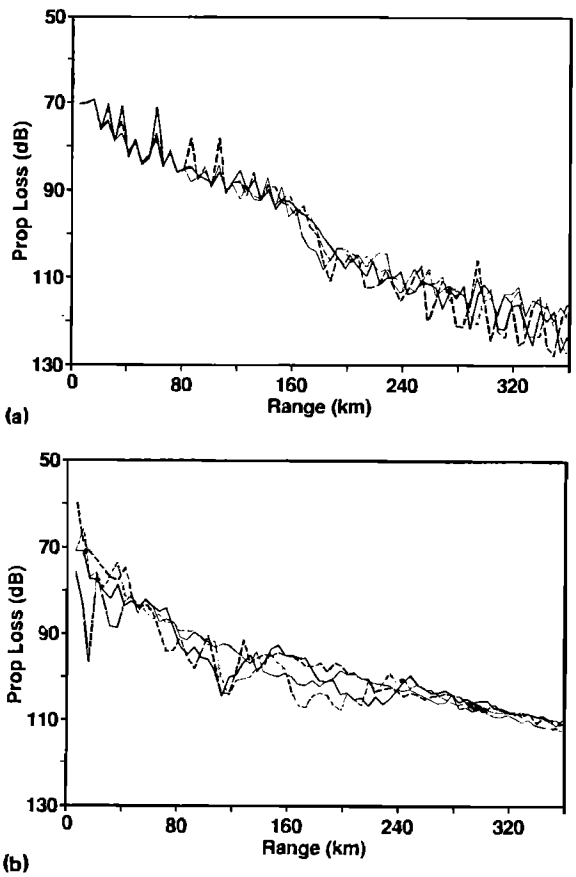

FIG. 10. Composite diagrams showing variation in calculated propagation loss on sections through (a) and (b) along the front $x = 120$ km and $y = 200$ km, respectively, and corresponding to horizontal eddy viscosity values of 2×10^7 (thin line), 1×10^7 (thin broken line), 0.5×10^7 (thick line), and 0.1×10^7 cm^2 s^{-1} (thick broken line). Here, K_H, K_V, and A_V were held constant at 10^5, 1, and 1 cm^2 s^{-1}, respectively.

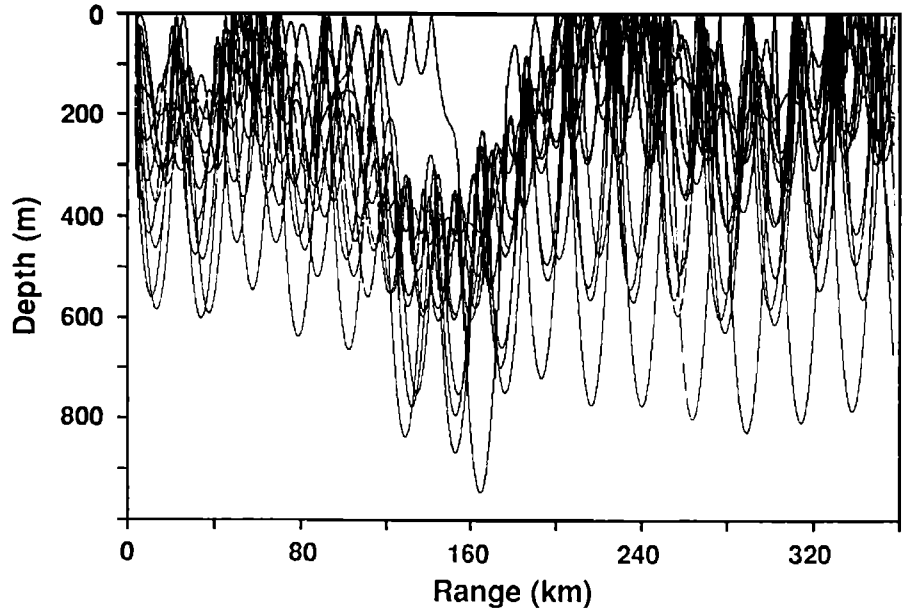

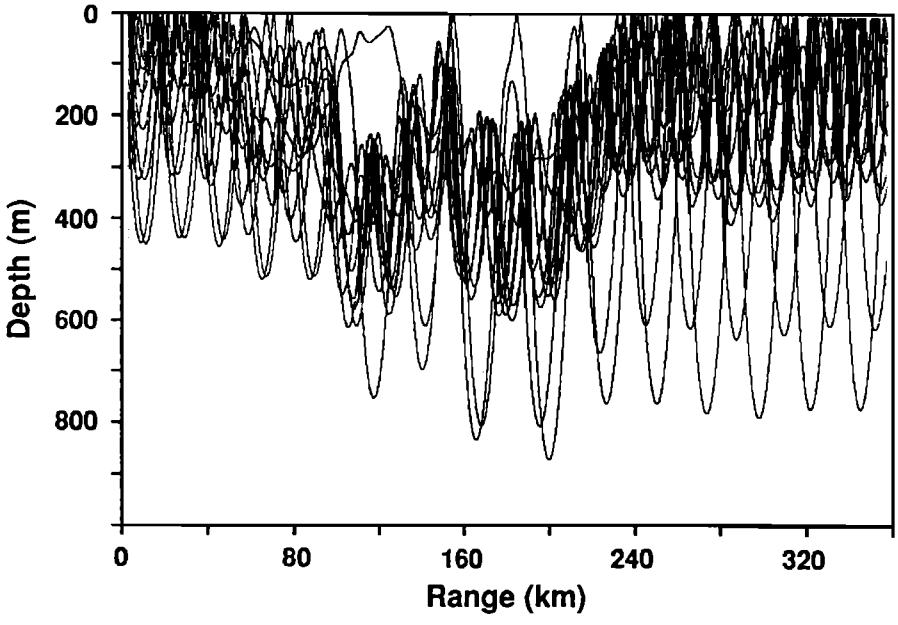

FIG. 11. Ray trace diagrams for the section along the front at $y = 200$ km and at 8 days following the initial baroclinic disturbance. The results illustrate the differences in the sound propagation paths at short ranges ($y < 40$ km) obtained with A_H values of (a) 0.1×10^7 cm^2 s^{-1}, and (b) 0.5×10^7 cm^2 s^{-1}, respectively.

ty of $\pm$ 5 dB that is associated with the spread of A_H used in the environmental simulations shown in Fig. 8. For sound propagating parallel to the front, the variations are of the order of $\pm$ 10 dB and are again associated with the spread of eddy viscosity values used in the ocean model simulations. For the situation examined here, the effects are particularly noticeable at short ranges, i.e., out to about 40 km. Figure 11 shows acoustic ray traces from ocean model simulations with A_H values of 0.1×10^7 cm^2 s^{-1} and 0.5×10^7 cm^2 s^{-1}, respectively, with the same initial disturbance and with the model integrated for 8 days. The differences at short ranges (< 40 km) are very apparent, as are the changes in the sound propagation paths at longer ranges around 140 km. Clearly, these differences will depend on the location of the sound source in relation to the ocean feature.

The range of A_H values that has been studied here is typical of the range of values used in other ocean model studies (e.g., Dippner[29] used $A_H = 0.3 \times 10^7$ cm^2 s^{-1}) and suggests that the acoustic calculations may be sensitive to the choice of ocean model parameter, in particular the value of the horizontal eddy viscosity coefficient, although we note that other forms of frictional and diffusive parametrization are possible (e.g., scale-selective biharmonic friction[30]) and that these may yield different results.

Despite these limitations, the acoustic models, when run on simulated environmental data from numerical ocean

models, have been found to give realistic estimates of the acoustic effects associated with ocean fronts and eddies. In particular, increases in propagation loss of up to 20 dB are predicted as a result of the frontal protrusions and eddylike features shown in Figs. 2, 3, and 8. This is of the same order as the frontal and eddy effect that is predicted from theoretical considerations[31,32] and comparable with values obtained from measurements at sea.

V. CONCLUSIONS

This study has demonstrated the feasibility of the coupled ocean-acoustic model technique with a 3-D primitive equation eddy resolving ocean model being used to provide environmental data for input to a range-dependent acoustic ray theory model. For this particular study, the ocean model has been configured so as to represent an idealized frontal system. The model was then perturbed baroclinically and integrated forward in time to generate eddy features having realistic spatial scales and growth rates. The principal conclusions of this study are (a) that for acoustic purposes a numerical ocean model is capable of giving realistic simulations of mesoscale eddy environments, and (b) that the underwater sound propagation characteristics (i.e., ray paths, propagation loss) that are calculated from these simulations are comparable to those which are predicted on the basis of measured environmental data and from theoretical considerations.

Of particular interest, ocean-acoustic model simulations have confirmed previous findings that ocean fronts and eddies may degrade sonar performance by as much as 20 dB. However, it has also been found that the acoustic predictions may be sensitive to the choice of ocean model parameter, in particular the horizontal eddy viscosity coefficient. Notwithstanding this difficulty, coupled ocean-acoustic models will allow variations in sonar performance to be studied, under well-controlled conditions, as a function of mesoscale variability on a range of spatial and temporal scales.

A further advantage is that the sensitivity of the acoustic predictions may be investigated as a function of both ocean model and acoustic model parameters. This information is of vital importance if acoustic models are to provide meaningful assessments of the outputs from Naval ocean forecast models.

ACKNOWLEDGMENTS

We are grateful to our colleagues at the Admiralty Research Establishment, Portland, for their assistance in the preparation of this paper. In particular, Bill Cooper and Roger Hillman assisted with earlier ocean-acoustic simulations.

[1] G. J. Kirby, "Some range dependent effects in sonar performance," Acoustics Bulletin, 12–15 (October 1988).
[2] N. L. Weinberg and J. G. Clark, "Horizontal acoustic refraction through ocean mesoscale eddies and fronts," J. Acoust. Soc. Am. **68**, 703–706 (1980).
[3] R. J. Urick, *Principles of Underwater Sound* (McGraw-Hill, New York, 1983).
[4] M. W. Lawrence, "Modeling of acoustic propagation across warm-core eddies," J. Acoust. Soc. Am. **73**, 474–485 (1983).
[5] R. F. Henrick, W. L. Siegmann, and M. J. Jacobson, "General analysis of ocean eddy effects for sound transmission applications," J. Acoust. Soc. Am. **62**, 860–870 (1977).
[6] R. F. Henrick, M. J. Jacobson, and W. L. Siegmann, "General effects of currents and sound speed variations on short range acoustic transmission in cyclonic eddies," J. Acoust. Soc. Am. **67**, 121–134 (1980).
[7] R. N. Baer, "Propagation through a three-dimensional eddy including the effects on an array," J. Acoust. Soc. Am. **69**, 70–75 (1981).
[8] T. H. Rousseau, W. L. Siegmann, and M. J. Jacobson, "Acoustic propagation through a model of shallow fronts in the deep ocean," J. Acoust. Soc. Am. **72**, 924–936 (1982).
[9] J. J. McManus, "Coupled mixed layer-acoustic model," M.S. thesis, Naval Postgraduate School, Monterery, California (1985).
[10] J. M. Fourniol, "Coupled acoustic and ocean thermodynamic model," M.S. thesis, Naval Postgraduate School, Monterery, California (1987).
[11] G. Botseas, D. Lee, and W. L. Siegmann, "IFD: Interfaced with Harvard open ocean model forecasts," Naval Underwater Systems Center, Report No. NUSC TR 8367 (1989).
[12] A. R. Robinson, "Dynamical forecasting of mesoscale fronts and eddies for acoustical applications," J. Acoust. Soc. Am. Suppl. 1 **82**, S2 (1987).
[13] S. M. Glenn and A. R. Robinson, "Nowcasting and forecasting of ocean dynamics and acoustic fields," to appear in *The Second IMACS Symposium on Computational Acoustics*, edited by D. Lee, A. Cakmac, and R. Vichnevetsky (North-Holland, Amsterdam, The Netherlands, 1990).
[14] W. L. Siegmann, M. J. Jacobson, D. Lee, G. Botseas, A. R. Robinson, and S. Glenn, "Interfacing mesoscale ocean prediction and parabolic acoustic propagation models," to appear in *The Second IMACS Symposium on Computational Acoustics*, edited by D. Lee, A. Cakmak, and R. Vichnevetsky (North-Holland, Amsterdam, The Netherlands, 1990).
[15] L. E. Mellberg, A. R. Robinson, and G. Botseas, "Modelled time variability of acoustic propagation through a Gulf Stream meander and eddies," J. Acoust. Soc. Am. **87**, 1044–1054 (1990).
[16] A. R. Robinson and L. J. Walstad, "The Harvard Open Ocean Model: Calibration and application to dynamical process, forecasting and data assimilation studies," Appl. Num. Math. **3**, 89–131 (1987).
[17] M. D. Cox, "A primitive equation, 3-dimensional model of the ocean," GFDL Ocean Group Tech. Rep. No. 1, Princeton University (1984).
[18] R. Bleck and D. B. Boudra, "Wind driven spin-up in eddy-resolving ocean models formulated in isopycnic and isobaric coordinates," J. Geophys. Res.**91C**, 7611–7621 (1986).
[19] A. D. Heathershaw, S. J. Maskell, W. St. J. Cooper and R. C. Hillman, "Studies of sound propagation through a front using an eddy resolving ocean model," Admiralty Res. Establishment Tech. Mem. (UJO) 88144, unpublished (1988).
[20] R. A. Wood, "Instability of oceanic fronts," Ph. D. thesis, University of Exeter, UK, unpublished (1988).
[21] D. P. Stevens, "On open boundary conditions for three dimensional primitive equation ocean circulation models," Geophys. Astron. Fluid Dyn. **51**, 103–133 (1990).
[22] W. St. J. Cooper, "Implementation of a 3-D ocean model," Admiralty Res. Establishment Tech. Mem. (UJO) 89125, unpublished (1989).
[23] J. Cornyn, "GRASS: A digital-computer ray-tracing and transmission loss prediction system. Vol. 1—Overall description", Naval Res. Lab. Rep. 7621 (1973).
[24] C. H. Harrison, "Ocean propagation models," Appl. Acoust. **27**, 163–201 (1989).
[25] C. T. Chien and F. J. Millero, "Speed of sound in sea water at high pressures," J. Acoust. Soc. Am. **62**, 1129 (1977).
[26] W. H. Thorp, "Deep-ocean sound attenuation in the sub and low-kilocycle-per-second region," J. Acoust. Soc. Am. **38**, 648–654 (1965).
[27] J. C. Scott and A. L. McDowall, "Cross-frontal cold jets near Iceland: In-water, satellite infra-red and GEOSAT altimeter data," J. Geophys. Res. (in press).
[28] P. D. Killworth, N. Paldor, and M. E. Stern, "Wave propagation and growth on a surface front in a two-layer geostrophic current," J. Marine Res. **42**, 761–785 (1984).
[29] J. W. Dippner, "Eddy-resolving modelling with dynamically active tracers," Cont. Shelf Res. **10**, 87–101 (1990).
[30] A. J. Semtner and R. M. Chervin, "A simulation of the global ocean circulation with resolved eddies," J. Geophys. Res. **93**, 15, 502-515, 522 (1988).
[31] R. N. Baer, "Calculations of sound propagation through an eddy," J. Acoust. Soc. Am. **67**, 1180–1185 (1980).
[32] S. Itzikowitz, M. J. Jacobson, and W. L. Siegmann, "Short-range acoustic transmissions through cyclonic eddies between a submerged source and receiver," J. Acoust. Soc. Am. **71**, 1131–1144 (1982).